VIROLOGY

Human TRA2A determines influenza A virus host adaptation by regulating viral mRNA splicing

Yinxing Zhu[1,2], Ruifang Wang[1,2]*, Luyao Yu[1,2], Huimin Sun[1,2], Shan Tian[1,2], Peng Li[1,2], Meilin Jin[1,2], Huanchun Chen[1,2], Wenjun Ma[3], Hongbo Zhou[1,2†]

Several avian influenza A viruses (IAVs) have adapted to mammalian species, including humans. To date, the mechanisms enabling these host shifts remain incompletely understood. Here, we show that a host factor, human TRA2A (huTRA2A), inhibits avian IAV replication, but benefits human IAV replication by altered regulation of viral messenger RNA (mRNA) splicing. huTRA2A depresses mRNA splicing by binding to the intronic splicing silencer motif in the M mRNA of representative avian YS/H5N1 or in the NS mRNA of representative human PR8/H1N1 virus, leading to completely opposite effects on replication of the human and avian viruses in vitro and in vivo. We also confirm that the M-334 site and NS-234/236 sites are critical for TRA2A binding, mRNA splicing, viral replication, and pathogenicity. Our results reveal the underlying mechanisms of adaptation of avian influenza virus to human hosts, and suggest rational strategies to protect public health.

INTRODUCTION

Aquatic birds are the main reservoir of most influenza A viruses (IAVs) in nature including identified H1-16 and N1-9 subtypes of viruses (*1*). It is very frequent that IAVs from their nature reservoir spill over to mammalian species, but very limited IAVs are able to adapt to and maintain in mammals including humans. When an IAV generated by reassortment or point mutations first accumulates sufficient adaptive mutations to sustain transmission between humans, it may result in a pandemic, as has been the case in 1918, 1957, 1968, and 2009 (*2*–*4*). The underlying mechanisms for adaptive changes in IAVs are still not completely understood.

IAV consists of eight negative single-strained RNA segments and three gene segments including *M*, *NS*, and *PB2* undergo alternative splicing (*5*, *6*). Alternative splicing of the M and NS segments produces two essential viral proteins each. The NS segment encodes the nonstructural protein (NS1) and nuclear export protein (NEP/NS2); the M segment encodes the matrix protein (M1) and ion channel (M2). Previous studies reveal that NEP plays an important role in regulating influenza virus polymerase activity and transcription and replication (*7*, *8*) and M2 is essential for virus budding (*9*). Although influenza virus transcribes and replicates the viral genome using the viral polymerase complex, it relies on numerous host factors to support their mRNA splicing (*10*); however, the detailed regulation mechanisms remain not completely understood.

The splicing of mRNA depends on the proper actions of both the spliceosome complex and splicing regulators, which is considered to be one of the most complex cellular processes (*11*). The splicing process is directed by numerous regulators including serine-arginine–rich (SR) proteins and heterogeneous nuclear ribonucleoproteins (hnRNPs) (*12*). The regulators bind to the cis-acting RNA splicing regulatory elements (SREs) that either positively or negatively influence splicing. SREs can be categorized as exonic splicing enhancers (ESEs), exonic splicing silencers, intronic splicing enhancers, and intronic splicing silencers (ISSs) depending on their locations and functions (*13*).

The splicing efficiency of the M and NS segments of IAVs could be a determining factor in their abilities to replicate or adapt to new hosts, suggesting an important role in pathogenicity (*14*–*16*). However, the relative accumulation of the *M1* and *NS1* gene products in human cells is completely different between human and avian influenza viruses (*17*), suggesting that their splicing in human and avian viruses may be different. Thus, unraveling the fine regulating mechanisms of viral splicing is imperative for a better understanding of viral replication, host range, and pathogenesis (*10*). Furthermore, why human and avian IAV splicing efficiency differs, which host factors are involved in host adaptation, and how and which splicing is related to host adaptation are needed to be addressed.

In this study, we revealed that a host factor, human TRA2A (huTRA2A), was able to bind to the ISS motif of either the M mRNA of avian IAV or the NS mRNA of human IAV and inhibited their splicing, but with opposite effects on virus replication of human and avian IAVs in vitro and in vivo. These results indicate that TRA2A-mediated alternative mRNA splicing is crucial for virus pathogenicity and adaption of influenza virus to humans.

RESULTS

TRA2A associates with viral ribonucleoprotein

A previous study has shown that the NP of PR8/H1N1 virus associates with TRA2A protein by using affinity purification mass spectrometry analysis (*18*). We first investigated whether TRA2A interacts with viral ribonucleoprotein (vRNP) complex that contains PA, PB1, PB2, NP, and viral RNA (vRNA), and results showed that the endogenous TRA2A coimmunoprecipitated with PA, PB1, PB2, and NP proteins under either human PR8/H1N1 (Fig. 1A) or avian YS/H5N1 (Fig. 1B) virus infection in A549 cells. Furthermore, results of RNA FISH (fluorescence in situ hybridization) and immunofluorescence assay showed that TRA2A colocalized with M vRNA (Fig. 1C) and NP protein (Fig. 1D) in the nucleus of both virus-infected A549 cells, respectively. These results indicate that TRA2A actually interacts and

[1]State Key Laboratory of Agricultural Microbiology, College of Veterinary Medicine, Huazhong Agricultural University, Wuhan 430070, China. [2]Key Laboratory of Preventive Veterinary Medicine in Hubei Province, Cooperative Innovation Center for Sustainable Pig Production, Wuhan 430070, China. [3]Department of Diagnostic Medicine/Pathobiology, Kansas State University, Manhattan, KS, USA.
*Present address: Department of Molecular Microbiology and Immunology, Keck School of Medicine, University of Southern California, Los Angeles, CA, USA.
†Corresponding author. Email: hbzhou@mail.hzau.edu.cn

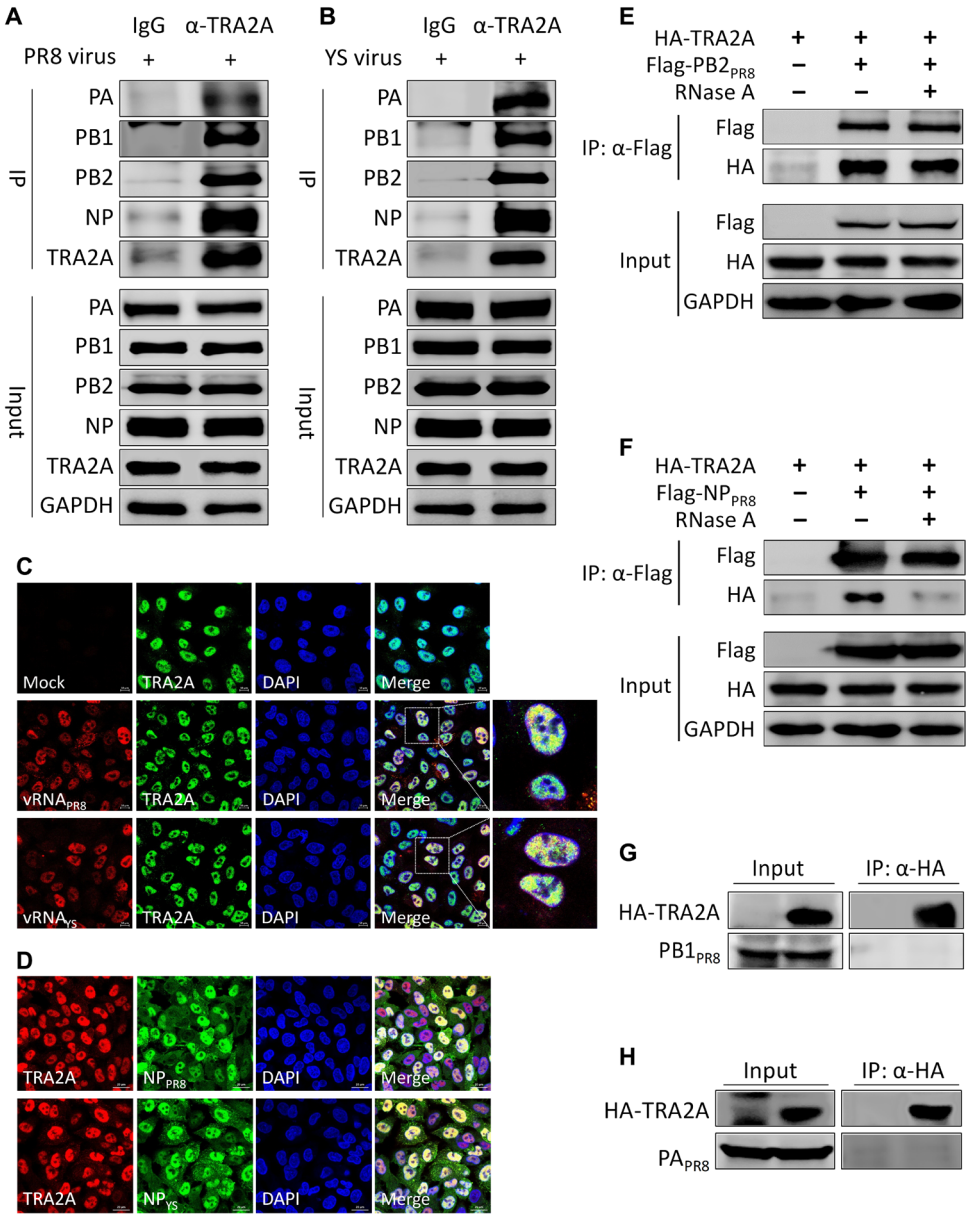

Fig. 1. TRA2A associates with vRNP. (**A** and **B**) A549 cells were infected with either the YS (A) or the PR8 (B) virus at a multiplicity of infection (MOI) of 0.01 for 24 hours; cell lysates were immunoprecipitated with an anti-TRA2A antibody or the control immunoglobulin G (IgG) and then analyzed by Western blotting. GAPDH, glyceraldehyde-3-phosphate dehydrogenase. (**C**) A549 cells were infected with the YS or PR8 virus at an MOI of 5. At 4 hours post-infection (hpi), cells were subjected to RNA FISH combined with immunofluorescence to detect M vRNA and TRA2A protein. Scale bars, 10 μm. DAPI, 4′,6′-diamidino-2-phenylindole. (**D**) A549 cells were infected with either YS or PR8 virus at an MOI of 0.01. At 24 hpi, cells were fixed and analyzed for the colocalization of TRA2A with NP. Scale bars, 20 μm. (**E** and **F**) Human embryonic kidney (HEK) 293T cells were transfected with the indicated plasmids for 24 hours. The cell lysates were treated with or without 100 U of ribonuclease A (RNase A) at 37°C for 1 hour. CoIP assay was performed using an anti-Flag antibody and analyzed by Western blotting. (**G** and **H**) HEK 293T cells were transfected with the indicated plasmids for 24 hours. Cell lysates were immunoprecipitated with an anti-hemagglutinin (HA) antibody and then analyzed by Western blotting.

colocalizes with vRNP. We next determined which specific component of vRNP binds to TRA2A. Coimmunoprecipitation (CoIP) assays showed that TRA2A only interacted with $PB2_{PR8}$ (Fig. 1E) and NP_{PR8} (Fig. 1F) but not $PB1_{PR8}$ (Fig. 1G) and PA_{PR8} (Fig. 1H). Moreover, immunofluorescence analysis revealed that PB2 and NP proteins from both viruses colocalized with TRA2A in the nucleus when they were coexpressed in A549 cells (fig. S1, A and B). As PB2 and NP associate with RNA, and TRA2A carries an RNA recognition motif (RRM) that is able to bind with RNA (*19*), we further determined whether the interaction between TRA2A and PB2 or NP is mediated by RNA. Results showed that the interaction between $PB2_{PR8}$ and TRA2A was RNA independent (Fig. 1E, line 3); in contrast, the interaction between TRA2A and NP_{PR8} was RNA dependent (Fig. 1F, line 3). Together, these results indicate that TRA2A interacts with vRNP but only interacts with PB2 and NP in the nucleus.

TRA2A inhibits avian influenza virus YS replication and promotes human influenza virus PR8 replication

We further tested whether huTRA2A affected PR8 or YS virus replication in A549 cells by median tissure culture infectious dose ($TCID_{50}$) assay and Western blot. As shown in Fig. 2A, knockdown TRA2A did not alter the cell viability at 36, 48, and 60 hours. Moreover, results showed that the virus titers and NP expression of YS were increased in TRA2A-knockdown (siTRA2A) cells (~0.5 $\log_{10}$ $TCID_{50}$ of virus titer, twofold of protein) (Fig. 2B) but obviously reduced in TRA2A overexpression cells at both 24 and 36 hpi (hours post-infection) in A549 cells (~0.5 $\log_{10}$ $TCID_{50}$) (Fig. 2C). In contrast, TRA2A knockdown suppressed PR8 replication at both 24 and 36 hpi (~0.75 $\log_{10}$ $TCID_{50}$) (Fig. 2D), whereas TRA2A overexpression resulted in enhancing virus replication (~1 $\log_{10}$ $TCID_{50}$) (Fig. 2E). We also performed the same experiments using the human glioma U251 cell line and showed that the results were consistent with those obtained in A549 cells (Fig. 2, F and G). Noticeably, overexpression of chicken TRA2A (chTRA2A) in A549 cells did not alter virus replication of avian virus (Fig. 2H). These results indicate that huTRA2A may have opposite effects on avian and human viruses' replication. To confirm that, we further revealed that the NP protein level was remarkably increased in TRA2A-knockdown cells infected with either the avian H9N2 (Fig. 2I, left) or H7N9 virus (Fig. 2I, middle), while a notable decrease was observed when infected with the human WSN/H1N1 virus (Fig. 2I, right). Together, these results indicate that huTRA2A but not chTRA2A is a restrictive factor for avian IAV replication but a positive factor for human IAV replication in human cells.

TRA2A inhibits YS-M and PR8-NS precursor mRNA splicing

To investigate whether TRA2A affects viral replication at the early stage of infection, we monitored the accumulation of virus proteins at 3, 6, and 9 hpi. Knockdown TRA2A increased the levels of PB1, NP, M1, M2, NS1, and NEP in YS-infected A549 cells compared with those in infected control-knockdown (siNC) cells (Fig. 3A), but completely opposite results were observed in PR8-infected cells (Fig. 3B). We observed the increased ratios of YS-M2/M1 (two and fivefold in 6 and 9 hours, respectively) and PR8-NEP/NS1 proteins (1.7- and 2.5-fold in 6 and 9 hours, respectively) in siTRA2A cells when compared to those in siNC cells infected with respective viruses. In contrast, the protein ratios of YS-NEP/NS1 and PR8-M2/M1 in both TRA2A- and NC-knockdown cells remained constant (Fig. 3, A and B).

The abnormal ratios of YS-M2/M1 and PR8-NEP/NS1 proteins suggest that TRA2A might negatively regulate the YS-M and PR8-NS mRNA splicing. The YS-M2/M1 mRNA ratio was notably increased (Fig. 3C), but the YS-NEP/NS1 mRNA ratio was not altered in TRA2A-knockdown cells (Fig. 3D). The PR8-M2/M1 mRNA ratio did not change (Fig. 3E), but the PR8-NEP/NS1 mRNA ratio was remarkably decreased (Fig. 3F). We performed above the same experiments on U251 cells and got the similar results as those obtained on A549 cells (fig. S2, A and B). In addition, we also used a semiquantitative method to detect splicing of M mRNA, and results showed that knockdown TRA2A was beneficial to YS-M splicing but did not change PR8-M splicing (Fig. 3G). However, overexpression of chTRA2A did not change the YS viral protein expression at different tested time points, suggesting that viral mRNA splicing was also not changed (fig. S2C). Together, our data indicate that TRA2A specifically inhibits the YS-M and PR8-NS mRNA splicing, leading to a completely opposite effect between human PR8 and avian YS virus replication.

TRA2A binds to the ISS motif of both YS-M and PR8-NS mRNA

We next determined how TRA2A targeted mRNA and inhibited splicing under virus infection. RNA immunoprecipitation (RIP) and reverse transcription quantitative polymerase chain reaction (RT-qPCR) analysis revealed that YS-M mRNA, but not control cellular RNA (U87), viral YS-NS, and YS-PB1 mRNA, was enriched more than eightfold by precipitation of TRA2A antibody in infected A549 cells in contrast to the control antibody [immunoglobulin G (IgG)] (Fig. 4A, left); furthermore, PR8-NS mRNA was enriched more than fivefold in comparison with both U87 and PR8-PB1 mRNA (Fig. 4A, right). A previous study has shown that TRA2A carries an RRM that is able to bind to the precursor mRNA bearing the purine-rich nucleotide motif GAAAR(G/A)GARR (*20*). We observed that the intron of both YS-M (nucleotides 334 to 343) and PR8-NS (nucleotides 233 to 242), but not of either YS-NS or PR8-M, carries this motif (Fig. 4B). Among them, the position 334 in YS-M is a guanine whereas the according position in PR8-M is a cytosine; there are two nucleotide differences (positions 234 and 236) in this motif between YS-NS and PR8-NS (Fig. 4B). To explore whether TRA2A binds with the YS-M and PR8-NS mRNA through this motif, we made a series of truncations (with or without the motif) and mutations (fig. S3, A and B). In vitro transcribed and labeled RNAs were incubated with nuclear extractions (NEs) under splicing conditions, and RNA pull-down assay was performed. Results showed that the endogenous TRA2A binds to the mRNAs of both PR8-NS_{Full} and PR8-$NS_{1–256}$, but not that of PR8-$NS_{1–232}$, PR8-$NS_{1–256(234G/236G)}$, YS-NS_{Full}, and its truncations (Fig. 4C). Moreover, TRA2A interacted with the mRNAs of both YS-M_{Full} and YS-$M_{1–360}$, but not with that of YS-$M_{1–333}$, YS-$M_{1–360(334C)}$, PR8-M_{Full}, and its truncations (Fig. 4E). These results revealed that the motif in YS-M and PR8-NS is essential for their binding with TRA2A. To further confirm that, RNA pull-down assay was performed by using the 20–base pair (bp) labeled probes containing respective motifs of either M or NS of each virus. Results showed that TRA2A protein preferably bound to the PR8-NS_{WT}, YS-$NS_{234A/236A}$, YS-M_{WT}, and PR8-M_{334G}, in comparison with the control pyrimidine-rich CU (cytosine and utracil) RNA, YS-NS_{WT}, PR8-$NS_{234G/236G}$, PR8-M_{WT}, and YS-M_{334C}, respectively (Fig. 4, D and F). Furthermore, electrophoretic mobility shift assay (EMSA) also revealed that the PR8-NS_{WT} probes bound with more TRA2A proteins than YS-NS_{WT} (Fig. 4G). The YS-M_{334C} mutation substantially decreased its binding to TRA2A (Fig. 4H, left), whereas the PR8-M_{334G} mutation showed the opposite results (Fig. 4H, right). Previous studies have shown that the host factor hnRNP K bound to M mRNA and promoted virus replication of human PR8 virus (*21*, *22*); we also found that the hnRNP K promoted avian virus replication (fig. S4A). To investigate whether the hnRNP K binding to M mRNA is influenced by TRA2A, we performed RIP assay. Results showed that M-334 mutation in YS did not change the binding of hnRNP K (fig. S4B), suggesting that the hnRNP K binding to the mRNA is not affected by TRA2A. Together, our results demonstrate that the GAAARGARR motif in YS-M and PR8-NS mRNAs is required for their association with huTRA2A; mutation at this motif disrupts the association. Because TRA2A can bind to the motif of YS-M and PR8-NS mRNAs and can inhibit their splicing, we define this motif as an ISS.

The ISS motif in M regulates its splicing and viral replication

To investigate the effect of the ISS motif in M on mRNA splicing and viral replication, we generated mutated viruses with YS-M_{334C}

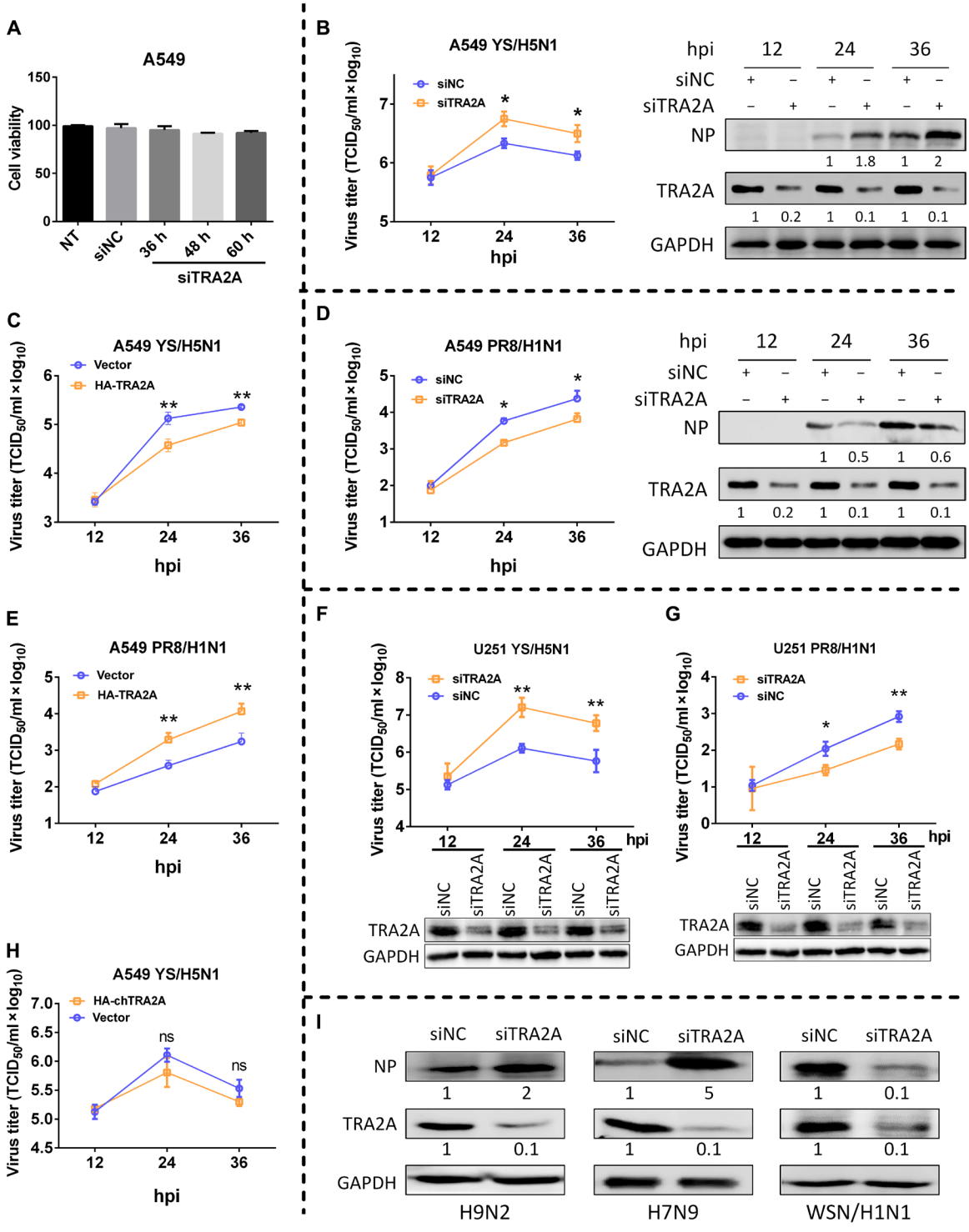

Fig. 2. TRA2A inhibits YS replication but enhances PR8 replication. (**A**) A549 cells were seeded on the 96-well plates, and cell viability was detected by Cell Counting Kit-8 assay at 36, 48, and 60 hours after transfection. NT, non-treated. (**B** to **H**) A549 (B to E and H) or U251 (F and G) cells were transfected with either HA-TRA2A, HA-chTRA2A, or pCAGGS vector or either siNC (negative control) or siTRA2A for 24 hours and then infected with the YS (B, C, F, and H) or PR8 (D, E, and G) virus at an MOI of 0.01. Cell culture supernatants were collected at 12, 24, and 36 hpi. Virus titers were determined by $TCID_{50}$ assay on MDCK (Madin-Darby canine kidney) cells. A549 cell lysates were analyzed by Western blotting, and the silence efficiency of TRA2A and changes of NP were quantified by ImageJ and normalized to GAPDH (C and E). (**I**) A549 cells were transfected with either siNC or siTRA2A for 24 hours and infected with an avian virus H9N2 or H7N9 or a human virus WSN/H1N1 strain at an MOI of 0.01. Cells lysates were subjected to Western blotting analysis. GAPDH was used as loading control. Each protein band was quantified by ImageJ and normalized to GAPDH levels. Means ± SD (error bars) of three independent experiments are indicated (*$P < 0.05$ and **$P < 0.01$).

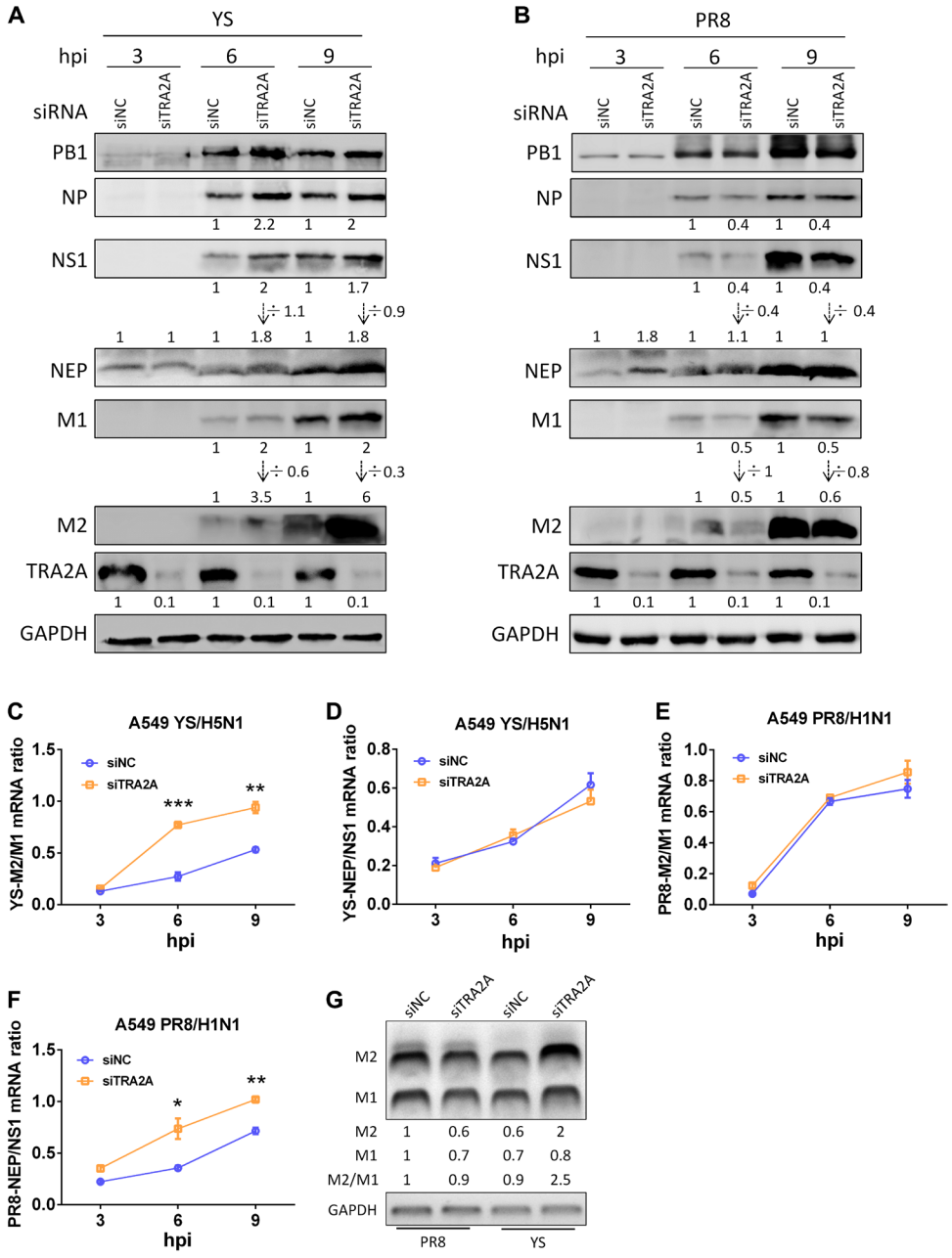

Fig. 3. TRA2A inhibit YS-M and PR8-NS mRNA splicing. (**A** to **G**) A549 cells were transfected with either siNC or siTRA2A for 24 hours and infected with the YS (A, C, D, and G) or PR8 (B and E to G) virus at an MOI of 5. Cell lysates were collected at 3, 6, and 9 hpi and subjected to Western blotting analysis. Each protein band was quantified by ImageJ and normalized to GAPDH levels. The NEP/NS1 and M2/M1 protein ratios were also calculated (A and B). The splicing ratios of M (C and E) and NS (D and F) mRNAs were analyzed by the specific reverse transcription quantitative polymerase chain reaction (RT-qPCR). The M2/M1 ratios were analyzed by semi-qPCR (G). Means ± SD (error bars) of three independent experiments are indicated (*$P < 0.05$, **$P < 0.01$, and ***$P < 0.001$).

and PR8-M_{334G} single mutation, respectively. The mutation in both viruses did not change the amino acid of M1 protein. In contrast to the avian YS-WT (wild-type) virus, the YS-M_{334C} virus infection resulted in increase of the mRNA levels of NP, M1, and M2 (Fig. 5A) and the M2/M1 mRNA ratio in human A549 cells (Fig. 5C) but not in DF1 chicken fibroblasts (fig. S5A). However, the mRNA levels of NP, M1, and M2 (Fig. 5B) and the M2/M1 mRNA ratio (Fig. 5D) were notably reduced in PR8-M_{334G} virus–infected human A549 cells compared to the PR8-WT–infected cells. We further determined whether the M-334 mutation altered their binding efficiency to TRA2A under virus infection. Results of RIP assay showed that the PR8-M_{334G} mRNA coimmunoprecipitated by endogenous TRA2A was twofold higher than that of PR8-WT (Fig. 5E, left), while the coimmunoprecipitated YS-WT mRNA was eightfold higher than the immunoprecipitated YS-M_{334C} mRNA (Fig. 5E, right). Moreover, the expression levels of PB2, NP, NS1, and M2 and the M2/M1

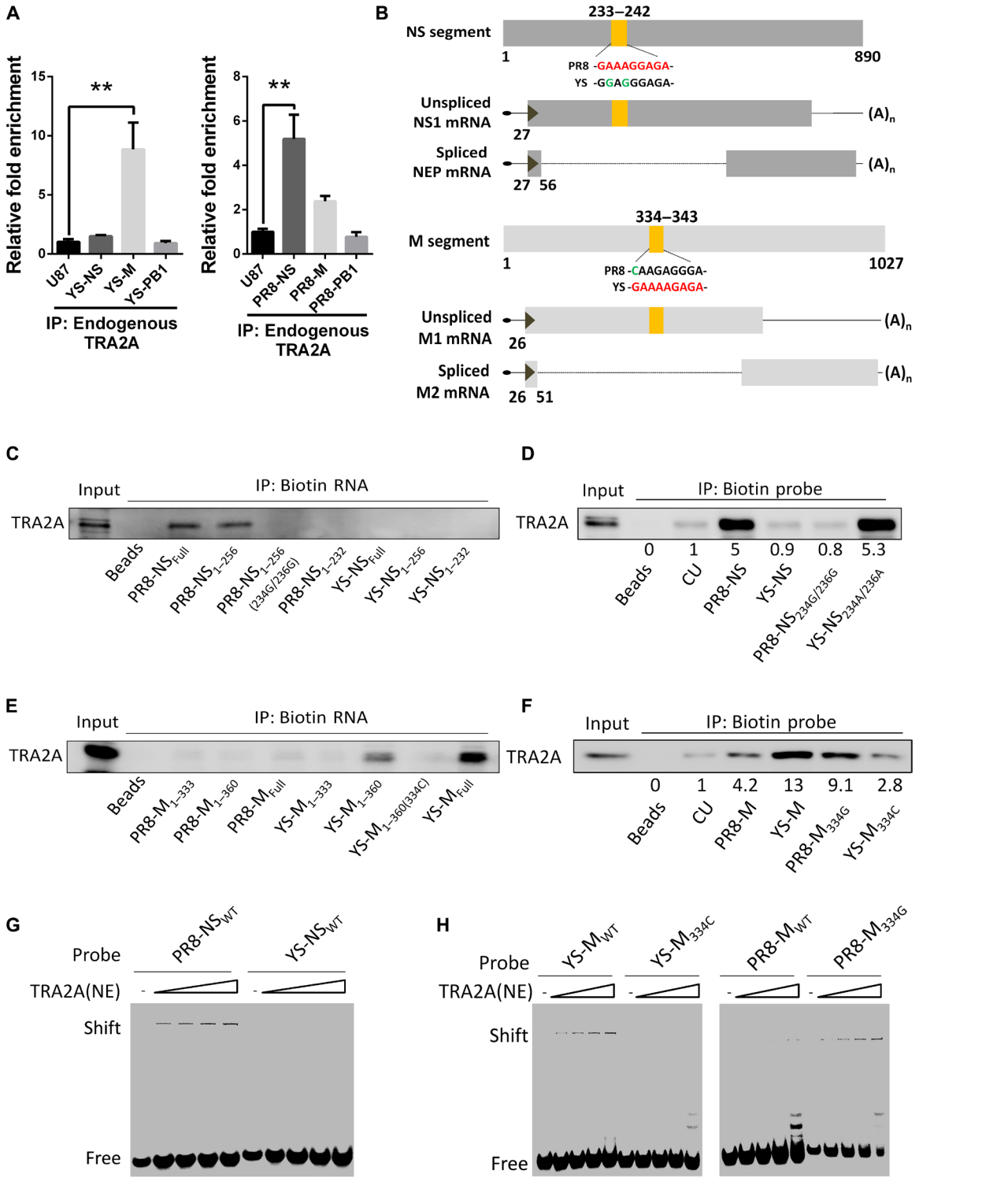

Fig. 4. TRA2A binds to the YS-M and PR8-NS mRNA through GAAARGARR motif. (**A**) A549 cells were infected with either the YS (left) or PR8 (right) virus at an MOI of 1 for 12 hours. RIPs and RT-qPCR were performed using specific primers detecting viral M, NS, and PB1 mRNA and cellular U87 small Cajal body-specific RNA (scaRNA). Fold enrichment of mRNA was calculated. Means ± SD (error bars) of three independent experiments are indicated (**$P < 0.01$). (**B**) Schematic illustration of the TRA2A binding sites in M and NS mRNA. (**C** and **E**) TRA2A bound to biotin-labeled YS or PR8 NS (C) or M (E) mRNAs or their truncated mRNAs. In vitro transcribed mRNAs were labeled with the biotin and immunoprecipitated with the NEs, and the bead eluate was then analyzed by Western blotting. (**D** and **F**) Pull-down TRA2A proteins using 20-bp NS (D) or M (F) biotin probes of PR8 and YS: Probes were immunoprecipitated with the NEs, and the bead eluate was analyzed by Western blotting. (**G**) TRA2A binding efficiency to PR8-NS_{WT} and YS-NS_{WT} was compared in RNA EMSA with increasing amounts of NEs. (**H**) TRA2A binding efficiency to YS-M_{WT} and YS-M_{334C} (left) and PR8-M_{WT} and PR8-M_{334G} (right) was compared in RNA EMSA with increasing amounts of NEs.

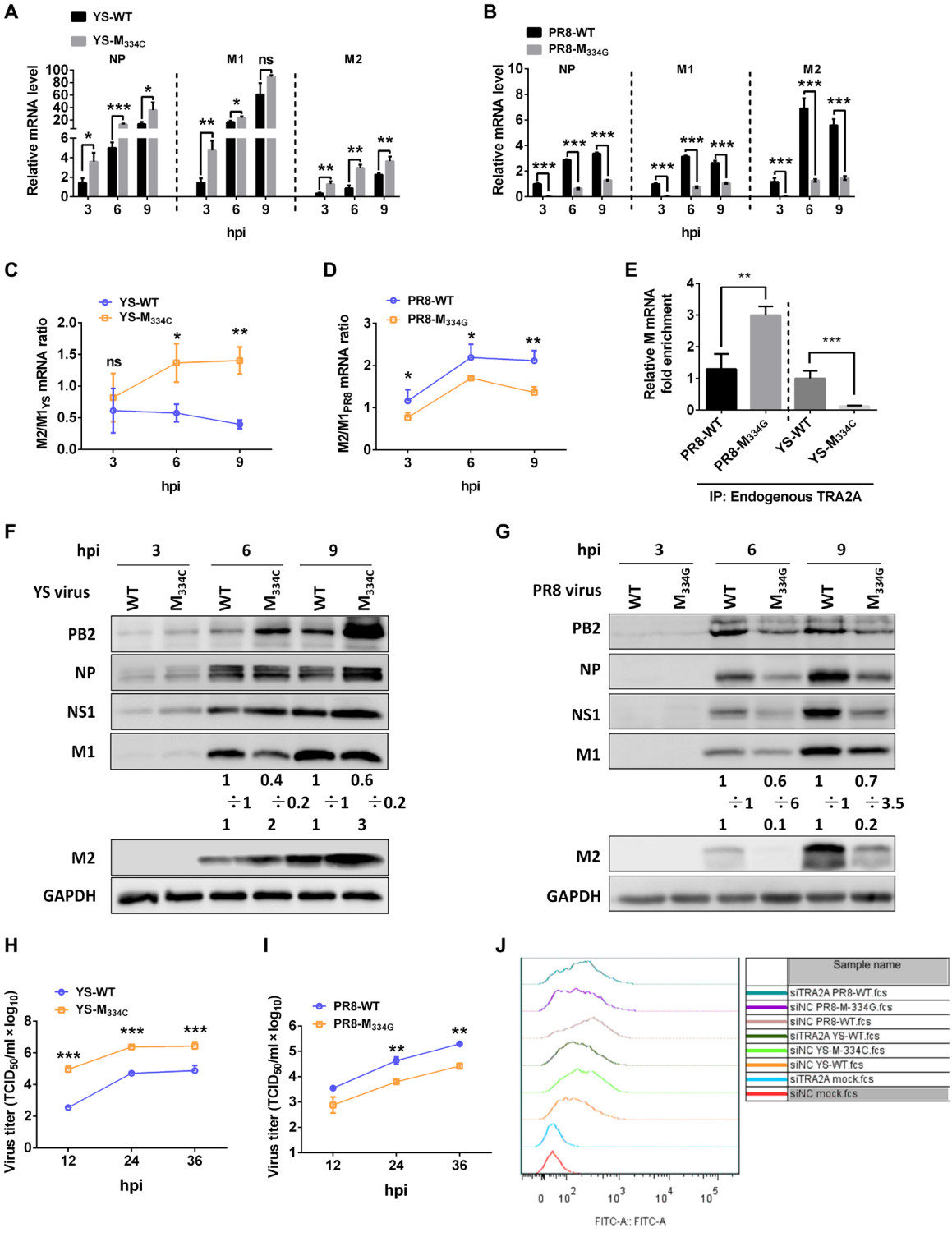

Fig. 5. M segment 334 site single mutation alters its mRNA splicing and virus replication. (**A** to **D**, **F**, and **G**) A549 cells were infected with either the PR8-WT, PR8-M_{334C}, YS-WT, or YS-M_{334C} virus at an MOI of 5; the total RNA was isolated and analyzed by RT-qPCR assay (A and B). Ratios of M2/M1 mRNA are presented (C and D). Cells lysates were subjected to Western blotting analysis using antibodies against respective influenza virus proteins. Each protein band was quantified by ImageJ and normalized to GAPDH levels (F and G). (**E**) A549 cells were infected with the WT or mutated YS (right) or PR8 (left) virus (MOI, 1) for 12 hours, and the mRNAs were purified with either the control IgG or the TRA2A antibody and analyzed by RT-qPCR assay. (**H** and **I**) Growth curves of the indicated virus. (**J**) A549 cells were transfected with siNC or siTRA2A for 24 hours and then infected with the indicated virus for 6 hours. Cells were stained with rabbit anti-HA antibody followed by fluorescein isothiocyanate (FITC)–goat anti-rabbit IgG and analyzed by flow cytometry. The data represent means ± SD (error bars) of three independent biological replicates (ns, not significant; $^{*}P < 0.05$, $^{**}P < 0.01$, and $^{***}P < 0.001$).

protein ratio were higher in the YS-M_{334C} virus–infected cells (Fig. 5F), whereas opposite results were found in the PR8-M_{334G} virus–infected cells (Fig. 5G) compared to their respective WT virus–infected cells. To assess the impacts of M-334 mutation on viral replication, we also compared the growth kinetics of the WT and mutated virus in A549, DF1, and DEF (duck embryonic fibroblast) cells. Results showed that the single mutation in YS-M_{334C} notably enhanced virus replication (~1.5 $\log_{10}$ $TCID_{50}$) in A549 cells (Fig. 5H) but not in either DF1 or DEF cells (fig. S5, B and C), whereas the single mutation in PR8-M_{334G} notably (~1 $\log_{10}$ $TCID_{50}$) decreased virus replication in A549 cells in contrast to their respective WT viruses (Fig. 5I).

We already demonstrated that ISS in M segment results in the production of less M2 (Fig. 3A). As M2 is crucial for viral budding (*9*), we investigated the hemagglutinin (HA) protein levels on cell membranes of live cells at 6 hpi. Results of flow cytometry showed that either knockdown TRA2A or mutated ISS in M changed virus budding (Fig. 5J and fig. S5D). Therefore, our results suggest that ISS mutation increases M2 production, thereby resulting in enhancing viral budding.

Together, these results indicate that restoring the ISS through single mutation in PR8-M_{334G} increases its binding with huTRA2A and restricts its mRNA splicing, resulting in lowering the ratio of M2/M1, thereby suppressing virus budding and replication in human cells. However, destroying the ISS via a single mutation in the YS-M_{334C} displays the opposite impacts in human cells but not in avian cells, suggesting that mutation of the ISS in avian influenza viruses is an important step to cross species barrier for adaptation to humans.

Single mutation at M-334 alters virus pathogenicity in mice

Given that the single mutation at position 334 in both YS-M and PR8-M altered their mRNA splicing and viral replication in human cells, we next determined the pathogenicity of the ISS mutated viruses in BALB/c mice. Results showed that the YS-M_{334C} virus infection notably enhanced pathogenicity while PR8-M_{334G} virus infection remarkably decreased virus pathogenicity when compared with their respective WT virus infection. Approximately 10- to 15-fold changes in the MLD_{50} (mouse median lethal dose) of each virus were observed (fig. S6, A to E). In addition, mice infected with YS-M_{334C} displayed severe weight loss and disease and 100% mortality, in comparison with those infected with the same dose of the YS-WT virus that caused 50% mortality (Fig. 6, A and B). In contrast, mice infected with PR8-M_{334G} showed slight weight loss and 50% mortality, while the PR8-WT resulted in severe disease and 80% mortality (Fig. 6, C and D).

The lungs of mice infected with either YS-M_{334C} or PR8-WT had moderate to severe bronchiolar necrosis, pulmonary edema, and inflammatory cell infiltrates, while the lung lymphoid tissue infiltration was restricted in either YS-WT or PR8-M_{334G}–infected mice at 3 dpi (days post-infection) (Fig. 6E). In addition, weaker NP antigen signals were detected in the lungs of mice infected with either YS-WT or PR8-M_{334G} virus when compared to those infected with either YS-M_{334C} or PR8-WT virus at 3 dpi (Fig. 6F). Virus titers in the lungs of mice infected with YS-M_{334C} were more than 20-fold higher at 3 dpi and more than 38-fold higher at 5 dpi than those detected in YS-WT–infected mice (Fig. 6G). However, virus titers in lungs of mice infected with PR8-WT were more than 30-fold higher at 3 dpi and over 4-fold higher at 5 dpi compared to those detected in mice infected with PR8-M_{334G} (Fig. 6G). To determine whether viral pathogenicity and replication in mice is related to the alteration of TRA2A binding, we detected the murine TRA2A binding to the M mRNA. Results showed that murine TRA2A prefers binding to the M mRNA with ISS (fig. S6F), similar to the hTRA2A, indicating that the level of binding to murine TRA2A is correlated with virus replication and virulence. These results indicate that destruction of ISS in M of the avian virus enhances viral pathogenicity in mammals, while restoring the ISS in M of the human virus reduces pathogenicity in mice, indicating that M-334 is a critical adaptive mutation for avian IAVs.

The ISS motif in PR8-NS regulates its splicing and viral replication

We also determined the effect of the ISS motif in PR8-NS on splicing, using reverse genetics to engineer ISS mutations in the background of PR8 virus. In contrast to the PR8-WT virus, the PR8-$NS_{234G/236G}$ mutations resulted in loss of the ISS and a notable reduction of the NP and NS1 mRNA (fig. S7A) and protein (fig. S7B) levels of NP and NS1. However, NEP mRNA and protein levels were not changed, resulting in the enhancement of NEP/NS1 ratio (fig. S7, B and C). Moreover, results of growth kinetics showed that the 234G/236G substitutions in PR8-NS notably decreased virus replication (~1 $\log_{10}$ $TCID_{50}$) compared to the WT viruses in A549 cells (fig. S7D). These results suggest that only a small amount of NEP is required for human IAV replication, while excessive NEP inhibits viral polymerase activity (fig. S7E). As TRA2A bound to the NS mRNA of PR8-WT rather than that of PR8-$NS_{234G/236G}$ in vitro (Fig. 4), we further investigated their interactions under virus infection in cells. As expected, the endogenous TRA2A coimmunoprecipitated with the NS mRNA of PR8-WT, which was 3.8-fold higher than the PR8-$NS_{234G/236G}$ (fig. S7F). Together, these results demonstrate that PR8-NS with the ISS increases TRA2A binding, which is not beneficial for its splicing, leading to less NEP protein production, thereby promoting human virus replication.

Furthermore, the PR8-M_{334G}-$NS_{234G/236G}$ double segment ISS mutations resulted in significantly decreased virus replication (~2 $\log_{10}$ $TCID_{50}$) when compared to either the PR8-WT or single-segment ISS mutated viruses (fig. S7G), suggesting that the ISS motifs in M and NS segments in PR8-WT virus play a synergistic role in virus replication.

TRA2A affects viral replication because of regulating mRNA splicing

We have shown that huTRA2A regulates M and NS splicing of representative avian and human influenza viruses, affecting virus replication (Fig. 3). To confirm the huTRA2A regulation of viral M and NS mRNA splicing resulting in the support or inhibition of viral replication, the huTRA2A-knockdown A549 cells were first infected with the ISS-mutated viruses including YS-M_{334C} and PR8-$NS_{234G/236G}$ to determine M and NS mRNA splicing in contrast to control cells. Results showed that the mRNA splicing of both ISS-mutated viruses did not change in TRA2A-knockdown cells (fig. S8, A and B). Furthermore, no difference in virus replication of mutated YS-M_{334G} and PR8-$NS_{234G/236G}$ viruses was observed in TRA2A-knockdown and control cells, while both PR8-WT and YS-WT viruses displayed markedly different growth dynamics in both cells (fig. S8, C and D). Thus, we conclude that TRA2A affects viral replication because of regulating mRNA splicing.

DISCUSSION

The genomes of IAVs are plastic, owing to point mutations and reassortment events that contribute to the emergence of new variants

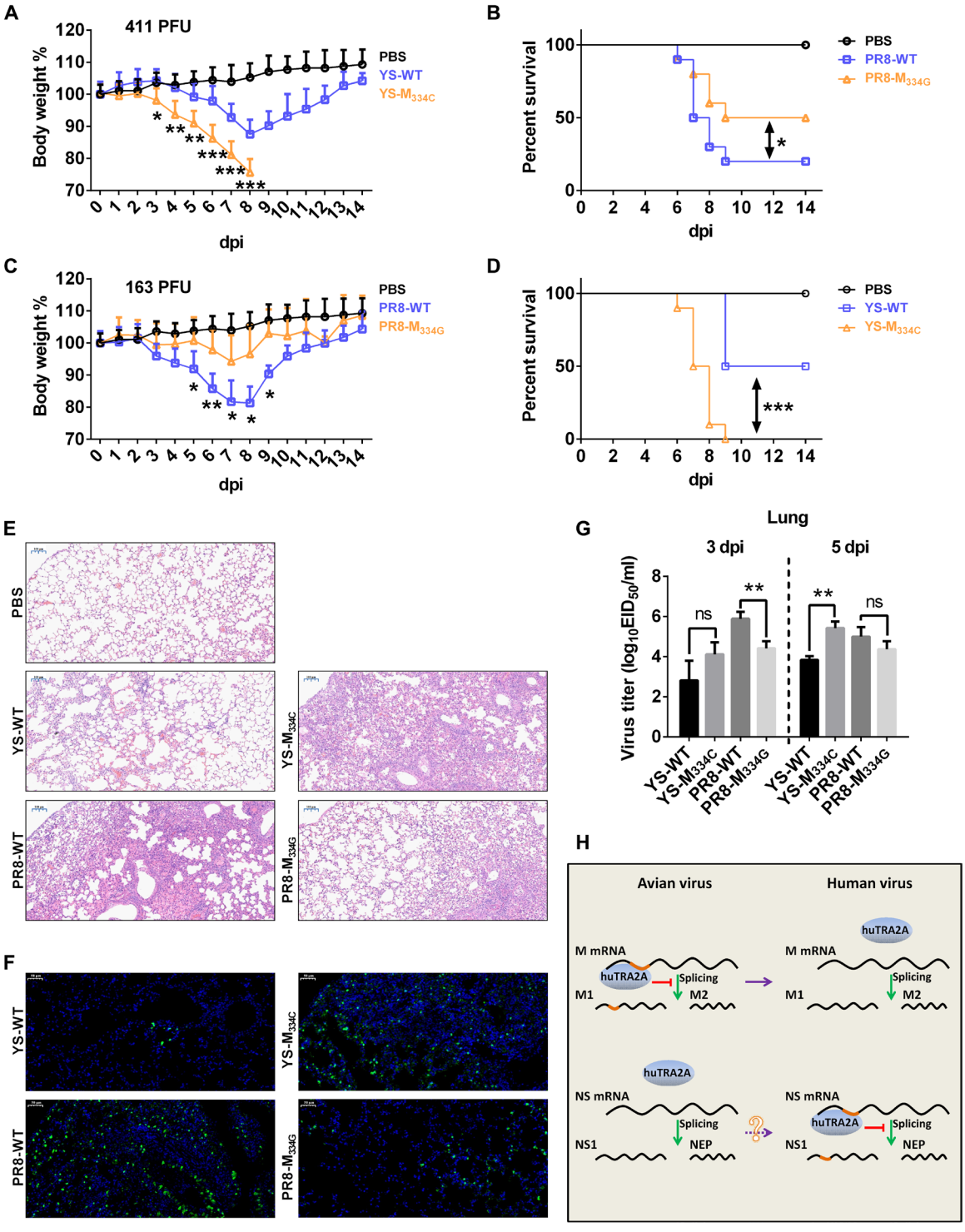

Fig. 6. Pathogenicity of WT YS or PR8 and their mutated viruses at 334 site in mice. Six-week-old female BALB/c mice were intranasally inoculated with the indicated doses of the PR8-WT, PR8-M_{334G}, YS-WT, or YS-M_{334C} virus or the phosphate-buffered saline (PBS) control. (**A** to **D**) Weight loss and mortality of mice infected with each indicted virus. Body weight of the WT and 334 mutant groups were compared and statistically analyzed. Error bars represent means ± SEM ($n = 10$). Statistical analysis was used by two-tailed analysis of variance (ANOVA) with Bonferroni post test. PFU, plaque-forming units. (**E**) Pathological lesions in the lungs of mice infected with the indicated virus at 3 dpi with hematoxylin and eosin (H&E) staining. Scale bars, 100 μm. (**F**) Immunofluorescent staining of lung sections of mice infected with the indicated virus at 3 dpi. The viral NP antigen was stained green, and the nucleus was stained blue. Scale bars, 50 μm. (**G**) Virus titers in the lungs of infected mice ($n = 3$) at 3 dpi (left) and 5 dpi (right). Error bars represent means ± SD. Statistical analysis was performed by using one-tailed method. EID_{50}, 50% egg infectious dose. (**H**) Model for avian IAV overcomes the huTRA2A host barrier. *$P < 0.05$, **$P < 0.01$, and ***$P < 0.001$.

or strains with epidemic or pandemic potential (*23*). Although avian IAVs including emerged H5N1 and H7N9 viruses were reported to have experienced reassortment or mutations to have abilities to cause human infections with a higher fatality (*24*–*27*), they could not gain human-to-human transmission and adapt to humans (*28*, *29*). In some rare cases, avian IAV can break through the host barrier and establish in the new host such as the Eurasian H1N1 swine influenza virus (*30*). In addition to adaptive mutations of viral genome, regulation of *M* and *NS* gene product expression through modulation of mRNA splicing is also implicated in influenza virus replication efficiency (*14*–*16*, *31*). In the present study, we provide solid evidence that both *M* and *NS* mRNAs splicing are critical for IAV replication and pathogenicity in human cells and in mice, indicating that it is also crucial for mammalian host adaptation.

The splicing of IAV mRNA is relying on the host's splicing system, and numerous splicing regulators involved in the regulation of IAV mRNA splicing have been identified, including splicing factor 2 (SF2), heterogeneous nuclear ribonucleoproteins K (hnRNP K), and influenza virus NS1 binding protein (NS1-B) (*22*, *32*, *33*). The mechanisms used by NS1-BP and hnRNP K positively regulating the M splicing of human virus (PR8) are that NS1-BP binds most proximal to the 5′ splice site and hnRNP K further binds downstream, promoting U1 small nuclear ribonucleoprotein recruitment, thereby enhancing the M mRNA splicing and virus replication (*21*, *32*, *34*). In this present study, we also find that the hnRNP K promotes avian virus replication (fig. S4A), suggesting that similar mechanisms could be used for both human and avian influenza viruses. SF2 not only regulates the NS mRNA splicing but also affects the M mRNA splicing by binding to the ESE in NEP or M2 (*22*, *33*). We identify the splicing regulator, huTRA2A, which restricts avian virus replication but benefits for human virus replication. The huTRA2A binds to the ISS motif of avian-*M* gene, resulting in inhibition of M mRNA splicing and unbalanced M2/M1 expression, thereby reducing avian virus replication and pathogenicity. When the ISS in the M of the avian virus was destroyed, virus replication and pathogenicity are enhanced. Although the ISS of M segment has been mutated, both hnRNP K and SF2 still bind to the M mRNA. This suggests that TRA2A does not influence their bindings to mRNA and is not directly involved in their regulation of mRNA splicing (fig. S4B). These results indicate that the mutation of ISS motif in the M is a critical adaptive step for avian influenza viruses. Recent studies have also proposed that the gene splicing of IAV M segment is related to virus transmissibility (*35*, *36*). Bogdanow and colleagues (*36*) show that avian virus produces less M1, while our studies reveal that avian virus produces less M2. These are most likely different virus strains used (an H3N2 avian virus used in their studies without the ISS in the M segment versus an H5N1 avian virus used in our studies with the ISS in the M segment). In contrast, the huTRA2A benefits human virus replication through inhibiting the human-NS mRNA splicing by binding to the ISS motif, inducing an unbalanced NS1 and NEP expression. When destruction of the ISS motif in the NS causes a relatively higher expression of NEP, it results in the inhibition of viral polymerase activity (fig. S7E) and replication. These results are in agreement with the findings of a previous study (*8*). However, the detailed mechanisms on how the NEP regulates the polymerase activity and virus replication need further investigations.

In nature, most human H1N1 and H3N2 IAVs do not carry ISS in their *M* genes but have the ISS motif in their *NS* segments (fig. S9, A and B). In contrast, normally, avian influenza viruses are opposite in both segments (fig. S9, A and B). The ISS in M segment of avian influenza virus plays a critical role in restricting the adaptation of avian influenza virus to mammals. We have identified three H5N1 human isolates A/Cambodia/Q0405047/2006, A/Vietnam/UT31394II/2008, and A/Vietnam/UT36250-1/2010, which have a mutated ISS in their *M* genes. In addition, we also observed that some avian H5N1, H7N9, H9N2, and H10N8 isolates have a mutated ISS in their *M* genes (fig. S9A), which could pose a potential threat to humans and require more attention to these ISS mutant viruses.

On the basis of the findings of our present study, when an avian influenza virus adapts to the new host such as humans, the ISS motif of their M and NS segments needs to be mutated so that huTRA2A is not able to bind to the M ISS motif but able to bind to the NS ISS motif, resulting in a balanced viral mRNA splicing as that of human IAVs (Fig. 6H). A markedly reduced virus replication was observed when introduction of the ISS motif into PR8-M and destruction of the ISS motif of PR8-NS was conducted, which suggests that modulation of both M and NS mRNA splicing plays a synergistic role in virus replication and adaption. Since the ISS motif in the NS segment was not detected in available avian influenza viruses so far and generation of ISS mutations in both M and NS segments in the YS virus might result in a gain-of-function study, we did not conduct similar studies for the PR8 virus.

A previous study has shown that the human, not avian, SF2 is able to regulate the NS mRNA splicing (*33*). In this present study, we reveal that huTRA2A, not avian, TRA2A regulate the M mRNA splicing (fig. S5, A to C). Which host factors in avian species and how they are involved in mRNA splicing and underlying mechanisms used remain unclear and need to be investigated. It has been documented that viral polymerases are able to directly or indirectly regulate IAV RNA splicing (*37*, *38*). A previous study has also shown that NS1-BP protein associates with the influenza virus polymerase subunit PB1 and regulates IAV M mRNA splicing (*32*). Our studies revealed that huTRA2A interacts with influenza vRNPs and specifically binds to NP and PB2 proteins (Fig. 1), suggesting that the viral polymerase may participate in viral mRNA splicing by interacting with splicing regulators. However, the mechanisms regarding how the viral polymerase is involved in regulation of viral mRNA splicing remain unknown and need to be further explored.

In summary, we identify a human host factor TRA2A associated with IAV mRNA splicing and reveal the underlying mechanism regarding IAV mRNA splicing, pathogenicity, and adaption to mammals such as humans. These findings could be used as a rational approach to develop live attenuated vaccine candidates to combat influenza.

MATERIALS AND METHODS

Ethics statements

This study was conducted in strict accordance with the recommendations provided in the *Guide for the Care and Use of Laboratory Animals* of the Ministry of Science and Technology of the People's Republic of China. Animal experiments were approved by the Hubei Administrative Committee for Laboratory Animals (approval no. SYXK-2010-0029).

Cells

HEK 293T, A549, U251, DF1, DEF, and MDCK (Madin-Darby canine kidney) cells were purchased from the American Type Culture Collection (Manassas, VA, USA), maintained in RPMI

1640 (HyClone, SH30809.01) medium or Dulbecco's modified Eagle's medium (Gibco, NY, USA) or Ham's/F-12 (HyClone, SH30026.01) medium supplemented with 10% heat-inactivated fetal bovine serum (522 PAN-Biotech, P30-3302), and incubated in 37°C humidified incubator with 5% CO_2.

Viruses and reverse genetics

Recombinant viruses were generated in the genetic background of either the PR8-WT or YS-WT virus using eight plasmid-based reverse genetic system as described previously (*39*). Eight segments of A/duck/Sheyang/1/2005 (H5N1) (YS) cloned into pHW2000 were obtained from D. Peng (Yangzhou University, Yangzhou, China), and eight segments of A/Puerto Rico/8/34 (H1N1) (PR8) were cloned into pHW2000 by our laboratory. Mutant *M* gene at position 334 and *NS* gene at positions 234 and 236 were generated by using a PCR-based site-directed mutagenesis. All constructs were confirmed by sequencing to ensure the absence of unwanted mutations. Recombinant viruses were propagated by single passage in embryonic chicken eggs. Virus stocks of WT and recombinant viruses were sequenced to confirm no additional mutations. All experiments with YS/H5N1 virus were performed in an animal biosafety level 3 laboratory of Huazhong Agricultural University.

Plasmids and small interfering RNA oligonucleotides

Full-length cDNA of huTRA2A, influenza viral *PA*, *PB1*, *PB2*, and *NP* genes of YS/H5N1 and PR8/H1N1 were amplified by RT-PCR from total RNA extracted from A549 cells infected with either YS or PR8 virus using specific primers and cloned into p3xFlag-CMV (Flag-PA/PB1/PB2/NP/NEP), HA-pCAGGS (HA-TRA2A), and pCDNA3.1-CMV (PA/PB1/PB2/NP), respectively. The vector pol-I-firefly was used for cloning NS. To generate mutant plasmids, site-directed mutagenesis was generated by using the QuikChange XL Site-Directed Mutagenesis Kit (Stratagene, La Jolla, CA) and overlap cloning techniques. Flag-SF2 was provided by H. Chen (The University of Hong Kong, Hong Kong), Flag-hnRNP K was provided by K. Guo (Huazhong Agricultural University, Wuhan). A549 and U251 cells were transfected with each small interfering RNA (siRNA) using Lipofectamine 2000 (Invitrogen) in accordance with the user manual for 24 hours before subsequent experiments. The primers and siRNA used in this study are shown in table S1.

Antibodies and reagents

Antibodies used in the study included the following: rabbit anti-TRA2A (GTX87998, GeneTex, USA); mouse anti-Flag (F1804, Sigma-Aldrich, Saint Louis, MO, USA); mouse anti–HA-tag (M180-3, MBL, Japan); mouse anti–glyceraldehyde-3-phosphate dehydrogenase (GAPDH) (CB100127, California Bioscience, Coachella, CA, USA); rabbit anti-IAV PA, PB1, PB2, NP, NS1, M1, NEP, M2, HA (GTX118991, GTX125923, GTX125926, GTX125989, GTX125990, GTX125928, GTX125953, GTX125951, and GTX127357, GeneTex, USA); mouse anti-NP (produced in our laboratory); control rabbit IgG polyclonal (AC005, ABclonal Biotechnology, Cambridge, MA, USA); horseradish peroxidase–conjugated anti-mouse and anti-rabbit (BF03001 and BF03008, Beijing Biodragon Inmmunotechnologies, China); Alexa Fluor 594-conjugated goat anti-rabbit (GR200G-43C, Sungene Biotech); fluorescein isothiocyanate (FITC)–goat anti-mouse (GM200G-02C, Sungene Biotech); and FITC-goat anti-rabbit (GR200G-02C, Sungene Biotech). 4′,6′-diamidino-2-phenylindole (1:1000) (no. C1002) was purchased from the Beyotime, China.

Coimmunoprecipitation and Western blotting

For RIP, A549 cells were infected with either PR8 or YS virus or their mutants at a multiplicity of infection (MOI) of 1 for 12 hours. Cell lysates were incubated with antibodies against either the TRA2A or control IgG antibodies at 4°C overnight and precipitated with Dynabeads (Sc-2003, Santa Cruz Biotechnology, USA) at room temperature for 30 min. After three washes with RIP buffer, RNAs were purified and analyzed by RT-qPCR. For protein CoIP, HEK 293T cells were cotransfected with indicated plasmids for 48 hours, or A549 cells were infected with the indicted virus at an MOI of 0.01; then, the cells were washed with cold phosphate-buffered saline (PBS) and lysed in cell lysis buffer for Western blotting and immunoprecipitation (P0013, Beyotime) containing protease inhibitor cocktail (04693132001, Roche, Basel, Switzerland). Cell lysates were incubated with antibody-bead complexes at 4°C overnight. Protein-antibody-bead complexes were washed three times with immunoprecipitation lysis buffer as described above. The complexes were then mock-treated or treated with ribonuclease A (Thermo Fisher Scientific, 12091039; 1:1000) at 37°C for 1 hour, washed three times, and analyzed by Western blotting.

RNA in vitro transcription, labeling, and pull-down assay

Full-length, 1-333, 1-360, and 1-360 mutant of M segment or full-length, 1-232, 1-256, and 1-256 mutant of NS segment were cloned into pCDNA3, which contained the T7 promoter. The cloned plasmids were linearized with the restriction enzyme Xba I. mRNA was synthesized by in vitro transcription with T7 RNA polymerase (M0251S, NEB, USA), and then, the DNA present in total RNA was eliminated by deoxyribonuclease (DNase) treatment (TaKaRa) in accordance with the user manual. mRNA was transcribed into cDNA by reverse transcriptase (AMV XL, TaKaRa, Japan), and then, mRNAs were labeled with biotin by using the Pierce RNA 3′ End Desthiobiotinylation Kit (20163, Thermo Fisher Scientific, USA). The labeled probes with biotin (TSINGKE Biological Technology, China) and labeled RNAs were incubated with A549 cell nuclear extracts; then, the RNA pull-down assay was performed using the Pierce Magnetic RNA-Protein Pull-Down Kit (20164, Thermo Fisher Scientific, USA). The proteins were analyzed by Western blotting.

RNA purification, RT-qPCR, and semi-qPCR

Total RNA was isolated from A549 cells with TRIzol Reagent (TaKaRa) according to the manufacturer's instructions. The DNA present in total RNA was eliminated by DNase treatment (TaKaRa) in accordance with the user manual. RNA was transcribed into cDNA by reverse transcriptase (AMV XL, TaKaRa, Japan). RT-qPCR (ABI ViiA7, USA) was performed using SYBR Green 1 (Roche). GAPDH expression was detected in each sample and used for normalization of gene expression between different samples. The PCR conditions were 2 min at 50°C, 10 min at 95°C, then 40 cycles of 15 s at 95°C, and 1 min at 60°C. The specificity of the assay was confirmed by melting curve analysis at the end of the amplification program (65°C to 95°C, $0.1°Cs^{-1}$). Semi-qPCR was performed using specific primers targeting *M1* and *M2* gene (table S1).

RNA EMSA

HEK 293T cells were harvested after 24 hours, washed by PBS, and lysed with sucrose buffer containing NP-40. Nuclear fraction was spun down and washed by sucrose buffer without NP-40. Nucleus pellets were resuspended in the low-salt buffer and incubated with

an equal volume of high-salt buffer for 30 min on ice, and NEs were prepared by spinning at 16,000*g* for 15 min. To set up the binding reaction, 10 nM of RNA probes (Nanjing Transcript, China) labeled with Cy5 at 5′ end were incubated with increasing doses of NE in 20 μl of buffered mixture [30 mM tris-HCl, 24 mM KCl, 800 mM $MgCl_2$, 0.008% NP-40, 3.3 mM dithiothreitol, 0.25% Tween 20, 4% glycerol, and 2 μg of yeast transfer RNA (pH 8.0)]. After incubation for 30 min at room temperature in the dark, mixtures were separated by 6.25% nondenaturing gel (0.5× tris-borate EDTA). Gels were scanned by an FLA-2000 fluorescent image analyzer (Fuji, Stamford, CT). RNA oligonucleotides used in RNA EMSA are listed in table S1.

Indirect immunofluorescence assay and confocal microscopy

Indirect immunofluorescence assay and confocal microscopy were performed as described in our previous study (*40*).

Growth kinetics of viruses

Cultures of A549 cells were transfected with indicated plasmids or siRNA. At 24 hours after transfection, cells were washed with Ham's/F-12 and infected with the indicated virus at an MOI of 0.01. The inoculums were removed after 1 hour of virus adsorption. Cells were then washed with Ham's/F-12 and cultured in minimal essential media containing N-tosyl-L-phenylalanine chloromethyl ketone (TPCK) trypsin (0.25 μg/μl). Supernatants of infected cells were collected at 12, 24, and 36 hpi and titrated on MDCK cells. Virus titers were determined by calculating $\log_{10}TCID_{50}$/ml using the Reed and Muench method.

Fluorescence in situ hybridization

FISH probes labeled with the Quasar 570 fluorophore for detecting PR8 H1N1 M segment vRNA were designed by using the online probe designer (Stellaris Probe Designer version 4.2). The probes were purchased from Biosearch Technologies (Novato, CA, USA). For in situ hybridization analysis, A549 cells infected with the PR8 or YS virus at an MOI of 5 in a 12-well plate were fixed for 10 min with 4% paraformaldehyde and then washed with PBS for three times. Cells were permeabilized with 0.2% Triton X-100 for 10 min and washed briefly. Next, cells were incubated with 200 μl of wash buffer A (SMF-WA1-60, Biosearch Technologies, USA) for 5 min. Wash buffer A was removed, and 300 μl of hybridization buffer (SMF-HB1-10, Biosearch Technologies, USA) containing 3 μl of FISH probes (final concentration, 12.5 nM) was added and incubated for 16 hours at 37°C in the dark. The hybridization buffer was removed, and cells were then incubated with wash buffer A for 5 min at 37°C. Images were obtained with a confocal microscope (LSM 880, ZEISS, Germany).

Pathogenicity study in mice

To determine MLD_{50} values, groups of five 6-week-old female BALB/c mice were lightly anesthetized with CO_2 and inoculated intranasally with 10-fold serial dilutions of PR8-WT, PR8-M_{334C}, YS-WT, or YS-M_{334G} in a volume of 50 μl. Mice were monitored daily for weight loss and mortality for 14 days. Mice that lost ≥20% of initial weight were humanely euthanized. MLD_{50} was calculated using the Reed and Muench method. To determine virus replication, groups of three BALB/c mice were intranasally inoculated with the indicated doses of PR8-WT, PR8-M_{334C}, YS-WT, or YS-M_{334G} diluted in PBS and were euthanized on 3 and 5 dpi. Virus titers in lungs collected from infected mice were determined in chicken embryonated eggs.

Polymerase assay

HEK 293T cells grown in 12-well plates were cotransfected with reporter plasmid pol-I-NS-firefly, virus polymerase, and NP plasmids (0.25 μg per well); plasmid pGL4.75 (0.02 μg per well; hRluc/CMV); and Flag-NEP_{PR8}–expressing plasmid (0.2, 0.4, or 0.8 μg per well) or an empty vector for 24 hours. Cells were lysed at 24 hours after transfection, and firefly luciferase and *Renilla* luciferase activities were determined using the Dual-Luciferase Reporter Assay System (Promega) according to the manufacturer's protocol. Data were presented as relative firefly luciferase activities normalized to *Renilla* luciferase activities and were representative of three independent experiments.

Statistical analysis

Virus titers in mouse tissues were statistically analyzed by one-tailed paired *t* test. Virus titers in A549 cells and other data were statistically analyzed by two-tailed paired *t* test.

SUPPLEMENTARY MATERIALS

Supplementary material for this article is available at http://advances.sciencemag.org/cgi/content/full/6/25/eaaz5764/DC1

View/request a protocol for this paper from *Bio-protocol*.

REFERENCES AND NOTES

1. R. G. Webster, W. J. Bean, O. T. Gorman, T. M. Chambers, Y. Kawaoka, Evolution and ecology of influenza a viruses. *Microbiol. Rev.* **56**, 152–179 (1992).
2. I. Wendel, M. Matrosovich, H. D. Klenk, SnapShot: Evolution of human influenza a viruses. *Cell Host Microbe* **17**, 416–416.e1 (2015).
3. M. Lipsitch, W. Barclay, R. Raman, C. J. Russell, J. A. Belser, S. Cobey, P. M. Kasson, J. O. Lloyd-Smith, S. Maurer-Stroh, S. Riley, C. A. Beauchemin, T. Bedford, T. C. Friedrich, A. Handel, S. Herfst, P. R. Murcia, B. Roche, C. O. Wilke, C. A. Russell, Viral factors in influenza pandemic risk assessment. *eLife* **5**, e18491 (2016).
4. J. S. Long, B. Mistry, S. M. Haslam, W. S. Barclay, Host and viral determinants of influenza a virus species specificity. *Nat. Rev. Microbiol.* **17**, 67–81 (2019).
5. P. Palese, M. Shaw, paper presented at the Fields Virology 6th edn, Philadelphia, PA, 2013.
6. S. Yamayoshi, M. Watanabe, H. Goto, Y. Kawaoka, Identification of a novel viral protein expressed from the PB2 segment of influenza a virus. *J. Virol.* **90**, 444–456 (2016).
7. B. Mänz, L. Brunotte, P. Reuther, M. Schwemmle, Adaptive mutations in NEP compensate for defective H5N1 RNA replication in cultured human cells. *Nat. Commun.* **3**, 802 (2012).
8. N. C. Robb, M. Smith, F. T. Vreede, E. Fodor, NS2/NEP protein regulates transcription and replication of the influenza virus RNA genome. *J. Gen. Virol.* **90**, 1398–1407 (2009).
9. H. Ma, F. Kien, M. Manière, Y. Zhang, N. Lagarde, K. S. Tse, L. L. M. Poon, B. Nal, Human annexin A6 interacts with influenza a virus protein M2 and negatively modulates infection. *J. Virol.* **86**, 1789–1801 (2012).
10. J. Dubois, O. Terrier, M. Rosa-Calatrava, Influenza viruses and mRNA splicing: Doing more with less. *MBio* **5**, e00070–e00014 (2014).
11. P. Papasaikas, J. Valcárcel, The Spliceosome: The Ultimate RNA chaperone and sculptor. *Trends Biochem. Sci.* **41**, 33–45 (2016).
12. J. Sperling, M. Azubel, R. Sperling, Structure and function of the pre-mRNA splicing machine. *Structure* **16**, 1605–1615 (2008).
13. X.-D. Fu, M. Ares Jr., Context-dependent control of alternative splicing by RNA-binding proteins. *Nat. Rev. Genet.* **15**, 689–701 (2014).
14. M. A. Chua, S. Schmid, J. T. Perez, R. A. Langlois, B. R. TenOever, Influenza A virus utilizes suboptimal splicing to coordinate the timing of infection. *Cell Rep.* **3**, 23–29 (2013).
15. E. Backström Winquist, S. Abdurahman, A. Tranell, S. Lindström, S. Tingsborg, S. Schwartz, Inefficient splicing of segment 7 and 8 mRNAs is an inherent property of influenza virus A/Brevig Mission/1918/1 (H1N1) that causes elevated expression of NS1 protein. *Virology* **422**, 46–58 (2012).
16. M. Selman, S. K. Dankar, N. E. Forbes, J.-J. Jia, E. G. Brown, Adaptive mutation in influenza A virus non-structural gene is linked to host switching and induces a novel protein by alternative splicing. *Emerg. Microbes Infect.* **1**, e42 (2012).
17. A. Sadewasser, K. Paki, K. Eichelbaum, B. Bogdanow, S. Saenger, M. Budt, M. Lesch, K. P. Hinz, A. Herrmann, T. F. Meyer, A. Karlas, M. Selbach, T. Wolff, Quantitative proteomic approach identifies Vpr binding protein as novel host factor supporting influenza a virus infections in human cells. *Mol. Cell. Proteomics.* **16**, 728–742 (2017).

18. L. Wang, B. Fu, W. Li, G. Patil, L. Liu, M. E. Dorf, S. Li, Comparative influenza protein interactomes identify the role of plakophilin 2 in virus restriction. *Nat. Commun.* **8**, 13876 (2017).
19. A. Best, C. Dalgliesh, M. Kheirollahi-Kouhestani, M. Danilenko, I. Ehrmann, A. Tyson-Capper, D. J. Elliott, Tra2 protein biology and mechanisms of splicing control. *Biochem. Soc. Trans.* **42**, 1152–1158 (2014).
20. M. Chen, J. L. Manley, Mechanisms of alternative splicing regulation: Insights from molecular and genomics approaches. *Nat. Rev. Mol. Cell Biol.* **10**, 741–754 (2009).
21. M. G. Thompson, R. Muñoz-Moreno, P. Bhat, R. Roytenberg, J. Lindberg, M. R. Gazzara, M. J. Mallory, K. Zhang, A. García-Sastre, B. M. A. Fontoura, K. W. Lynch, Co-regulatory activity of hnRNP K and NS1-BP in influenza and human mRNA splicing. *Nat. Commun.* **9**, 2407 (2018).
22. S. R. Shih, R. M. Krug, Novel exploitation of a nuclear function by influenza virus: The cellular SF2/ASF splicing factor controls the amount of the essential viral M2 ion channel protein in infected cells. *EMBO J.* **15**, 5415–5427 (1996).
23. G. Neumann, T. Noda, Y. Kawaoka, Emergence and pandemic potential of swine-origin H1N1 influenza virus. *Nature* **459**, 931–939 (2009).
24. M. Imai, T. Watanabe, M. Hatta, S. C. Das, M. Ozawa, K. Shinya, G. Zhong, A. Hanson, H. Katsura, S. Watanabe, C. Li, E. Kawakami, S. Yamada, M. Kiso, Y. Suzuki, E. A. Maher, G. Neumann, Y. Kawaoka, Experimental adaptation of an influenza H5 HA confers respiratory droplet transmission to a reassortant H5 HA/H1N1 virus in ferrets. *Nature* **486**, 420–428 (2012).
25. C. A. Russell, J. M. Fonville, A. E. Brown, D. F. Burke, D. L. Smith, S. L. James, S. Herfst, S. van Boheemen, M. Linster, E. J. Schrauwen, L. Katzelnick, A. Mosterín, T. Kuiken, E. Maher, G. Neumann, A. D. Osterhaus, Y. Kawaoka, R. A. Fouchier, D. J. Smith, The potential for respiratory droplet-transmissible A/H5N1 influenza virus to evolve in a mammalian host. *Science* **336**, 1541–1547 (2012).
26. L. Cui, D. Liu, W. Shi, J. Pan, X. Qi, X. Li, X. Guo, M. Zhou, W. Li, J. Li, J. Haywood, H. Xiao, X. Yu, X. Pu, Y. Wu, H. Yu, K. Zhao, Y. Zhu, B. Wu, T. Jin, Z. Shi, F. Tang, F. Zhu, Q. Sun, L. Wu, R. Yang, J. Yan, F. Lei, B. Zhu, W. Liu, J. Ma, H. Wang, G. F. Gao, Dynamic reassortments and genetic heterogeneity of the human-infecting influenza A (H7N9) virus. *Nat. Commun.* **5**, 3142 (2014).
27. A. Wu, C. Su, D. Wang, Y. Peng, M. Liu, S. Hua, T. Li, G. F. Gao, H. Tang, J. Chen, X. Liu, Y. Shu, D. Peng, T. Jiang, Sequential reassortments underlie diverse influenza H7N9 genotypes in China. *Cell Host Microbe* **14**, 446–452 (2013).
28. X. Wang, P. Wu, Y. Pei, T. K. Tsang, D. Gu, W. Wang, J. Zhang, P. W. Horby, T. M. Uyeki, B. J. Cowling, H. Yu, Assessment of human-to-human transmissibility of avian influenza A(H7N9) virus across 5 waves by analyzing clusters of case patients in Mainland China, 2013-2017. *Clin. Infect. Dis.* **68**, 623–631 (2019).
29. H. Wang, Z. Feng, Y. Shu, H. Yu, L. Zhou, R. Zu, Y. Huai, J. Dong, C. Bao, L. Wen, H. Wang, P. Yang, W. Zhao, L. Dong, M. Zhou, Q. Liao, H. Yang, M. Wang, X. Lu, Z. Shi, W. Wang, L. Gu, F. Zhu, Q. Li, W. Yin, W. Yang, D. Li, T. M. Uyeki, Y. Wang, Probable limited person-to-person transmission of highly pathogenic avian influenza A (H5N1) virus in China. *Lancet* **371**, 1427–1434 (2008).
30. R. J. Garten, C. T. Davis, C. A. Russell, B. Shu, S. Lindstrom, A. Balish, W. M. Sessions, X. Xu, E. Skepner, V. Deyde, M. Okomo-Adhiambo, L. Gubareva, J. Barnes, C. B. Smith, S. L. Emery, M. J. Hillman, P. Rivailler, J. Smagala, M. de Graaf, D. F. Burke, R. A. M. Fouchier, C. Pappas, C. M. Alpuche-Aranda, H. López-Gatell, H. Olivera, I. López, C. A. Myers, D. Faix, P. J. Blair, C. Yu, K. M. Keene, P. D. Dotson Jr., D. Boxrud, A. R. Sambol, S. H. Abid, K. S. George, T. Bannerman, A. L. Moore, D. J. Stringer, P. Blevins, G. J. Demmler-Harrison, M. Ginsberg, P. Kriner, S. Waterman, S. Smole, H. F. Guevara, E. A. Belongia, P. A. Clark, S. T. Beatrice, R. Donis, J. Katz, L. Finelli, C. B. Bridges, M. Shaw, D. B. Jernigan, T. M. Uyeki, D. J. Smith, A. I. Klimov, N. J. Cox, Antigenic and genetic characteristics of swine-origin 2009 A(H1N1) influenza viruses circulating in humans. *Science* **325**, 197–201 (2009).
31. M. Zheng, P. Wang, W. J. Song, S.-Y. Lau, S. Liu, X. Huang, B. W.-Y. Mok, Y.-C. Liu, Y. Chen, K.-Y. Yuen, H. L. Chen, An A14U substitution in the 3' noncoding region of the M segment of viral RNA supports replication of influenza virus with an NS1 deletion by modulating alternative splicing of M segment mRNAs. *J. Virol.* **89**, 10273–10285 (2015).
32. P.-L. Tsai, N.-T. Chiou, S. Kuss, A. García-Sastre, K. W. Lynch, B. M. A. Fontoura, Cellular RNA binding proteins NS1-BP and hnRNP K regulate influenza A virus RNA splicing. *PLOS Pathog.* **9**, e1003460 (2013).
33. X. Huang, M. Zheng, P. Wang, B. W.-Y. Mok, S. Liu, S.-Y. Lau, P. Chen, Y.-C. Liu, H. Liu, Y. Chen, W. Song, K.-Y. Yuen, H. Chen, An NS-segment exonic splicing enhancer regulates influenza A virus replication in mammalian cells. *Nat. Commun.* **8**, 14751 (2017).
34. A. Mor, A. White, K. Zhang, M. Thompson, M. Esparza, R. Muñoz-Moreno, K. Koide, K. W. Lynch, A. García-Sastre, B. M. A. Fontoura, Influenza virus mRNA trafficking through host nuclear speckles. *Nat. Microbiol.* **1**, 16069 (2016).
35. B. M. Calderon, S. Danzy, G. K. Delima, N. T. Jacobs, K. Ganti, M. R. Hockman, G. L. Conn, A. C. Lowen, J. Steel, Dysregulation of M segment gene expression contributes to influenza A virus host restriction. *PLOS Pathog.* **15**, e1007892 (2019).
36. B. Bogdanow, X. Wang, K. Eichelbaum, A. Sadewasser, I. Husic, K. Paki, M. Budt, M. Hergeselle, B. Vetter, J. Hou, W. Chen, L. Wiebusch, I. M. Meyer, T. Wolff, M. Selbach, The dynamic proteome of influenza A virus infection identifies M segment splicing as a host range determinant. *Nat. Commun.* **10**, 5518 (2019).
37. G. Fournier, C. Chiang, S. Munier, A. Tomoiu, C. Demeret, P.-O. Vidalain, Y. Jacob, N. Naffakh, Recruitment of RED-SMU1 complex by influenza A Virus RNA polymerase to control viral mRNA splicing. *PLOS Pathog.* **10**, e1004164 (2014).
38. S. R. Shih, M. E. Nemeroff, R. M. Krug, The choice of alternative 5′ splice sites in influenza virus M1 mRNA is regulated by the viral polymerase complex. *Proc. Natl. Acad. Sci. U.S.A.* **92**, 6324–6328 (1995).
39. E. Hoffmann, G. Neumann, Y. Kawaoka, G. Hobom, R. G. Webster, A DNA transfection system for generation of influenza A virus from eight plasmids. *Proc. Natl. Acad. Sci. U.S.A.* **97**, 6108–6113 (2000).
40. R. Wang, Y. Zhu, X. Lin, C. Ren, J. Zhao, F. Wang, X. Gao, R. Xiao, L. Zhao, H. Chen, M. Jin, W. Ma, H. Zhou, Influenza M2 protein regulates MAVS-mediated signaling pathway through interacting with MAVS and increasing ROS production. *Autophagy* **15**, 1163–1181 (2019).

Acknowledgments: We thank W. S. Barclay (Imperial College, London) for helpful discussions and comments. We also thank Y. Tao (Rice University, Houston), X. Xiong (MRC Laboratory of Molecular Biology, Cambridge), and X. Xiao (Huazhong Agricultural University, China) for critically proofreading the manuscript. **Funding:** This work was supported by the National Natural Science Foundation of China (31761133005 and 31772752) and the National Key Research and Development Program (2016YFD0500205). **Author contributions:** Y.Z., W.M., and H.Z. designed the experiments and analyzed data. Y.Z., R.W., W.M., and H.Z. wrote the paper. Y.Z., R.W., L.Y., H.S., and S.T. performed the experiments and organized data. Y.Z., R.W., and P.L. contributed reagents/materials/analysis tools. All authors discussed the results and read the manuscript. **Competing interests:** The authors declare that they have no conflict of interest. **Data and materials availability:** All data needed to evaluate the conclusions in the paper are present in the paper and/or the Supplementary Materials. Additional data related to this paper may be requested from the authors.

Submitted 20 September 2019
Accepted 28 April 2020
Published 19 June 2020
10.1126/sciadv.aaz5764

Citation: Y. Zhu, R. Wang, L. Yu, H. Sun, S. Tian, P. Li, M. Jin, H. Chen, W. Ma, H. Zhou, Human TRA2A determines influenza A virus host adaptation by regulating viral mRNA splicing. *Sci. Adv.* **6**, eaaz5764 (2020).